COUPLED LATERAL AND TORSIONAL FAILURE OF BUILDINGS UNDER TWO-DIMENSIONAL EARTHQUAKE SHAKINGS

H. Takizawa (I)

SUMMARY

The nature of structural failure caused under significant influence of torsion is studied by accounting for the two-dimensional effects of excitation and restoring force relation. From novel points of view, the examinations begin with an instructive note on the modal properties of torsionally coupled systems and a tensorial formulation for the response deformation developed on the horizontal plane. Important features in the behavior close to ultimate failure are then illustrated by means of a planar distribution of reinforced concrete biaxial elements. Their yielding and hysteretic modeling in two dimensions includes additional factors of cracking and cyclic stiffness degradation.

INTRODUCTION

Since early days in the study of structural dynamics for earthquake engineering, torsional effects have attracted intense concern in assessing the safety of building structures. Notable contributions can be found in the past literature of torsionally coupled response, practical implications of which have tended to be reflected upon existing standards of aseismic design. However the current state of the art appears to be still unsatisfactory for purposes of describing important features in the behavior close to ultimate failure. Necessity of considerable improvements is specifically felt in such points as the biaxial interaction of yielding and hysteretic restoring forces, and the 2-D (two-dimensional) action of earthquake shakings on the horizontal plane. In particular, methods for reinforced concrete biaxial systems must allow to account for the marked softening associated with cracking and the degrading capacity of cyclic energy loss as well as the post-yield deterioration of ductility. With these factors in mind, the present report investigates the nature of structural failure sustained under significant role of torsion.

Throughout the presentation, examinations place emphasis on deformation rather than force. This begins with an instructive note on the modal properties of torsionally coupled elastic systems. A tensor formulation follows to aid the better understanding of response deformation developed on the horizontal plane. The subsequent illustration is chosen to highlight trends in the structural failure of lateral and torsional coupling which occurs under a 2-D ground motion. The example system consists of a planar distribution of restoring force elements by means of the reinforced concrete biaxial model formulated previously by the author.

FEATURES IN EIGENPROBLEM

Art. (1) indicates the equation of motion for single-story rigid-floor systems subjected to 2-D ground shakings [Fig. 1-(a)], components of the inertia and stiffness matrices in which can be simplified into Art. (1'). The first noteworthy point is an equivalent expression of the combined lateral and torsional stiffness matrix. As shown in Art. (2), this is based on a novel

(I) *Associate Professor of Structural Engineering, Faculty of Engineering, Hokkaido University, Sapporo, Japan.*

(1) $[M]\{\ddot{D}(t)\} + (\text{damping term}) + [K]\{D(t)\} = -[M][\{E_x\}\ddot{D}_{x0}(t) + \{E_y\}\ddot{D}_{y0}(t)]$

where

$$\{D(t)\} = \begin{Bmatrix} D_x(t) \\ D_y(t) \\ \theta(t) \end{Bmatrix} \qquad \{E_x\} = \begin{Bmatrix} 1 \\ 0 \\ 0 \end{Bmatrix} \qquad \{E_y\} = \begin{Bmatrix} 0 \\ 1 \\ 0 \end{Bmatrix}$$

$$[M] = \begin{bmatrix} M & 0 & -y_g M \\ 0 & M & x_g M \\ -y_g M & x_g M & (i_m^2 + x_g^2 + y_g^2)M \end{bmatrix}$$

M : total inertia of the system

(x_g, y_g) : position of gravity center, G

i_m : radius of gyration with respect to G

$$[K] = \begin{bmatrix} [K_{tt}] & [K_{tt}]\{s\} \\ \lfloor s \rfloor [K_{tt}] & K_\theta + \lfloor s \rfloor [K_{tt}]\{s\} \end{bmatrix}$$

$[K_{tt}]$: translational stiffness matrix with respect to S

$$\{s\} = \begin{Bmatrix} -e_y \\ e_x \end{Bmatrix} \qquad (e_x, e_y) : \text{position of shear center, S}$$

K_θ : torsional stiffness with respect to S

(1')

$$[M] = \begin{bmatrix} M & 0 & 0 \\ 0 & M & 0 \\ 0 & 0 & i_m^2 M \end{bmatrix} \qquad [K] = \begin{bmatrix} K_x & 0 & -e_y K_x \\ 0 & K_y & e_x K_y \\ -e_y K_x & e_x K_y & K_\theta + e_y^2 K_x + e_x^2 K_y \end{bmatrix}$$

when locating the origin of coordinate frame at G, and the x and y axes along the principal axes of $[K_{tt}]$

(2) When $e_x \neq 0$ and $e_y \neq 0$ (biaxially eccentric),

$$[K] = \begin{bmatrix} K_0 + K_{wx} & 0 & -e_{wy}K_{wx} \\ 0 & K_0 + K_{wy} & e_{wx}K_{wy} \\ -e_{wy}K_{wx} & e_{wx}K_{wy} & i_m^2 K_0 + e_{wy}^2 K_{wx} + e_{wx}^2 K_{wy} \end{bmatrix}$$

where K_0 : "isotropic and homogeneous reference stiffness", which is the least eigenvalue satisfying

$$\det\left(\begin{bmatrix} K_x & 0 & -e_y K_x \\ 0 & K_y & e_x K_y \\ -e_y K_x & e_x K_y & K_\theta + e_y^2 K_x + e_x^2 K_y \end{bmatrix} - K_0 \begin{bmatrix} 1 & 0 & 0 \\ 0 & 1 & 0 \\ 0 & 0 & i_m^2 \end{bmatrix} \right)$$

$= 0$, and falls within the region of $K_0 < \min(K_x, K_y)$.

$$\left.\begin{matrix} K_{wx} = K_x - K_0 \\ K_{wy} = K_y - K_0 \end{matrix}\right\} : \text{components of "concentrated eccentric stiffness"}$$

$$\left.\begin{matrix} e_{wx} = e_x K_y/(K_y - K_0) \\ e_{wy} = e_y K_x/(K_x - K_0) \end{matrix}\right\} (e_{wx}, e_{wy}) : \text{position of "eccentricity center of stiffness", W}$$

When $e_x \neq 0$ and $e_y = 0$ (uniaxially eccentric),

$$[K] = \begin{bmatrix} K_x & 0 & 0 \\ 0 & K_0 + K_{wy} & e_{wx}K_{wy} \\ 0 & e_{wx}K_{wy} & i_m^2 K_0 + e_{wx}^2 K_{wy} \end{bmatrix}$$

where

$$\det\left(\begin{bmatrix} K_y & e_x K_y \\ e_x K_y & K_\theta + e_x^2 K_y \end{bmatrix} - K_0 \begin{bmatrix} 1 & 0 \\ 0 & i_m^2 \end{bmatrix} \right) = 0 \qquad (K_0 < K_y)$$

$$K_{wy} = K_y - K_0 \qquad e_{wx} = e_x K_y/(K_y - K_0)$$

(3)

$$\Omega(x, y) = \sqrt{\frac{K_\theta + (y - e_y)^2 K_x + (x - e_x)^2 K_y}{(i_m^2 + x^2 + y^2)M}}$$

: circular frequency of oscillation when specifying a twisting center at (x, y)

(4) For biaxially eccentric cases,

$$\left(-{}_s\Omega^2 \begin{bmatrix} M & 0 & 0 \\ 0 & M & 0 \\ 0 & 0 & M \end{bmatrix} + \begin{bmatrix} K_0 + K_{wx} & 0 & -\bar{e}_{wy}K_{wx} \\ 0 & K_0 + K_{wy} & \bar{e}_{wx}K_{wy} \\ -\bar{e}_{wy}K_{wx} & \bar{e}_{wx}K_{wy} & K_0 + \bar{e}_{wy}^2 K_{wx} + \bar{e}_{wx}^2 K_{wy} \end{bmatrix} \right) \begin{Bmatrix} {}_s\bar{e}_y \\ -{}_s\bar{e}_x \\ 1 \end{Bmatrix} = \{0\}$$

$\bar{e}_{wx} = e_{wx}/i_m \qquad \bar{e}_{wy} = e_{wy}/i_m$

${}_s\bar{e}_x = {}_s e_x/i_m \qquad {}_s\bar{e}_y = {}_s e_y/i_m$

$({}_s e_x, {}_s e_y)$: position of the rotational center in the s-th mode, ${}_s E$

$$M\,{}_1\Omega^2 = K_0$$

$$\left.\begin{matrix} M\,{}_2\Omega^2 \\ M\,{}_3\Omega^2 \end{matrix}\right\} = K_0 + \frac{1}{2}\left[(1+\bar{e}_{wy}^2)K_{wx} + (1+\bar{e}_{wx}^2)K_{wy} \mp \sqrt{\{(1+\bar{e}_{wy}^2)K_{wx} - (1+\bar{e}_{wx}^2)K_{wy}\}^2 + 4\bar{e}_{wx}^2\bar{e}_{wy}^2 K_{wx}K_{wy}} \right]$$

$${}_1\bar{e}_x = \bar{e}_{wx}$$

$${}_1\bar{e}_y = \bar{e}_{wy}$$

$$\left.\begin{matrix} {}_2\bar{e}_x \\ {}_3\bar{e}_x \end{matrix}\right\} = \frac{-(1+\bar{e}_{wy}^2)K_{wx} + (1-\bar{e}_{wx}^2)K_{wy} \mp \sqrt{\{(1+\bar{e}_{wy}^2)K_{wx} - (1+\bar{e}_{wx}^2)K_{wy}\}^2 + 4\bar{e}_{wx}^2\bar{e}_{wy}^2 K_{wx}K_{wy}}}{2\bar{e}_{wx}(K_{wx} - K_{wy})}$$

$$\left.\begin{matrix} {}_2\bar{e}_y \\ {}_3\bar{e}_y \end{matrix}\right\} = \frac{-(1-\bar{e}_{wy}^2)K_{wx} + (1+\bar{e}_{wx}^2)K_{wy} \pm \sqrt{\{(1+\bar{e}_{wy}^2)K_{wx} - (1+\bar{e}_{wx}^2)K_{wy}\}^2 + 4\bar{e}_{wx}^2\bar{e}_{wy}^2 K_{wx}K_{wy}}}{2\bar{e}_{wy}(K_{wx} - K_{wy})}$$

$${}_s e_x\,{}_t e_x + {}_s e_y\,{}_t e_y + i_m^2 = 0 \qquad (s \neq t)$$

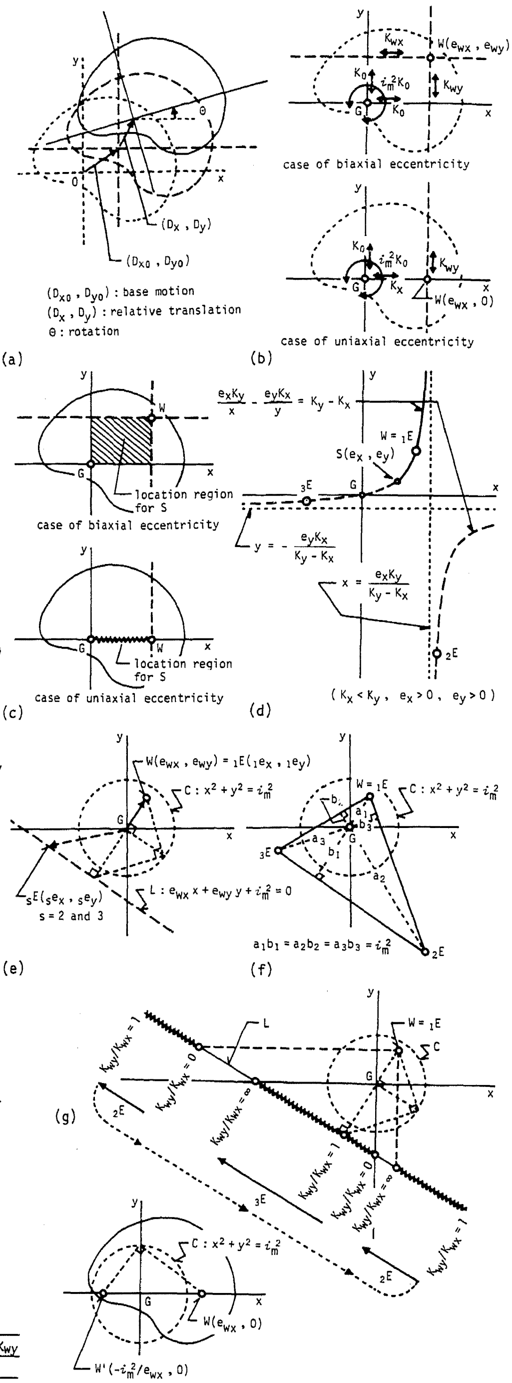

Figure 1

definition of "isotropic and homogeneous reference stiffness", K_0, and two components of "concentrated eccentric stiffness", K_{wx} and K_{wy}. The corresponding planar distribution of stiffness appears in Fig. 1-(b), a geometry concerning the three centers of gravity, shear and "concentrated eccentricity" (G, S and W) being included in Fig. 1-(c).

A geometrical interpretation of the associated eigenvalue problem is provided by examining the variation of the natural frequency of oscillation according to the movement of a specified center of twist on the plane. By use of the formula in Art. (3), Fig. 2 gives an example where the extremal nature of eigenvalues (concave, saddle and convex points) is appealingly seen. This line of thinking leads to an interesting finding concerning the limitation imposed on the position of eigencenters with relation to G and S [Fig. 1-(d)]. The hyperbolic law becomes of a particular importance for the fundamental eigencenter, ${}_1E$.

Art. (4) shows the algebraic eigenproblem in terms of the equivalent expression of stiffness matrix for biaxial eccentricity. The components of eigenvectors are represented there by means of the position of eigencenters. It is immediately seen that K_0 is directly responsible for the fundamental eigenvalue, ${}_1E$ coinciding with W. Moreover, role of K_0 is completely isolated in higher eigenvalues. Rendered independent of K_0, factors to determine the position of higher eigencenters are reduced to the position of W and the relative value between K_{wx} and K_{wy}. The same article also includes the modal orthogonality relationships expressed in terms of the position of eigencenters, from which the following instructive properties of elementary geometry can be derived. Given the inertia circle, C, and the position of W, higher eigencenters turn out to lie on a line, L, whose drawing procedure is indicated in Fig. 1-(e). A pair of L and the symmetric point of W against G is the so-called polar and pole with respect to C in the theories of quadratic curves. The three eigencenters form an "acute" triangle, whose orthocenter is G [Fig. 1-(f)]. More specifically, location of higher eigencenters on L can be characterized by the changing value of K_{wy}/K_{wx} as suggested in Fig. 1-(g). On the other hand, the condition of uniaxial eccentricity yields far simpler properties [Fig. 1-(h)]. The

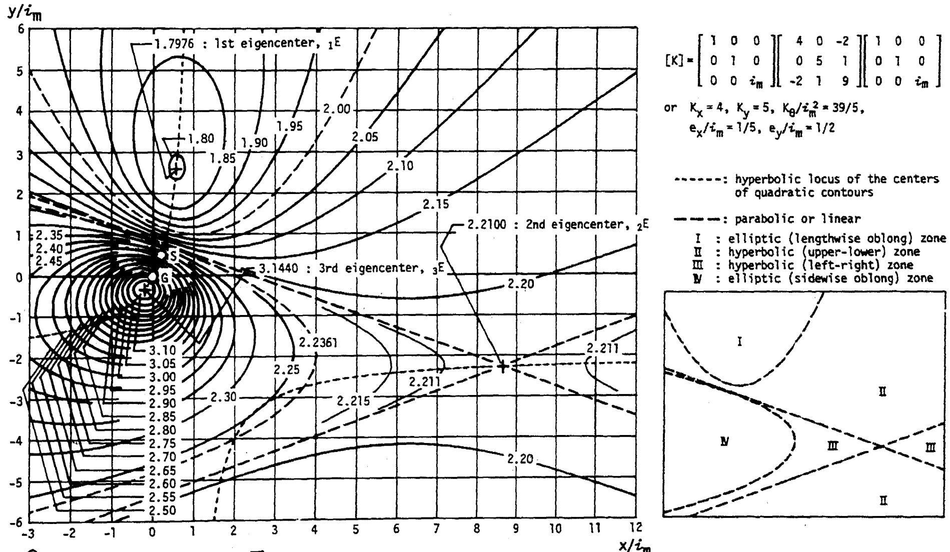

Figure 2 Contour curves of $\sqrt{M}\,\Omega(x,y)$

two eigencenters may be considered as a conjugate pair with respect to C. In addition, Art. (5) supplements the formulas of modal decomposition. Participation functions are specified therein by use of the position of eigencenters.

The equation of motion takes a form of Art. (6) for multi-story systems. Consider particular cases in which system characteristics are ideally separable between the plane and the storywise axis as defined in Art. (7). Art. (9) indicates the eigensolution including modal participation functions can be then obtained as a simple combination of the separate planar and axial solutions of Art. (8). Therefore the preceding properties of single-story systems can be readily extended to this family of multi-story systems.

(5)
$$\begin{Bmatrix} d_x(x,y,t) \\ d_y(x,y,t) \end{Bmatrix} = \begin{bmatrix} 1 & 0 & -y \\ 0 & 1 & x \end{bmatrix} \begin{Bmatrix} D_x(t) \\ D_y(t) \\ \Theta(t) \end{Bmatrix} = \sum_{s=1}^{3} \begin{bmatrix} {}_s(\beta u)_{xx}(x,y) & {}_s(\beta u)_{xy}(x,y) \\ {}_s(\beta u)_{yx}(x,y) & {}_s(\beta u)_{yy}(x,y) \end{bmatrix} \begin{Bmatrix} {}_sf_x(t) \\ {}_sf_y(t) \end{Bmatrix}$$

where
$$\begin{bmatrix} {}_s(\beta u)_{xx}(x,y) & {}_s(\beta u)_{xy}(x,y) \\ {}_s(\beta u)_{yx}(x,y) & {}_s(\beta u)_{yy}(x,y) \end{bmatrix} = \frac{1}{1+{}_s\bar{e}_x^2+{}_s\bar{e}_y^2} \begin{bmatrix} {}_s\bar{e}_y({}_s\bar{e}_y-\bar{y}) & -{}_s\bar{e}_x({}_s\bar{e}_y-\bar{y}) \\ {}_s\bar{e}_y(-{}_s\bar{e}_x+\bar{x}) & -{}_s\bar{e}_x(-{}_s\bar{e}_x+\bar{x}) \end{bmatrix}$$
$$(\bar{x}=x/i_m,\ \bar{y}=y/i_m)$$

$$\sum_{s=1}^{3} \begin{bmatrix} {}_s(\beta u)_{xx}(x,y) & {}_s(\beta u)_{xy}(x,y) \\ {}_s(\beta u)_{yx}(x,y) & {}_s(\beta u)_{yy}(x,y) \end{bmatrix} \equiv \begin{bmatrix} 1 & 0 \\ 0 & 1 \end{bmatrix}$$

$$\begin{Bmatrix} {}_s\ddot{f}_x(t) \\ {}_s\ddot{f}_y(t) \end{Bmatrix} + 2\,{}_s\zeta\,{}_s\Omega \begin{Bmatrix} {}_s\dot{f}_x(t) \\ {}_s\dot{f}_y(t) \end{Bmatrix} + {}_s\Omega^2 \begin{Bmatrix} {}_sf_x(t) \\ {}_sf_y(t) \end{Bmatrix} = -\begin{Bmatrix} \ddot{D}_{x0}(t) \\ \ddot{D}_{y0}(t) \end{Bmatrix}$$

${}_s\zeta$: viscous damping factor in the s-th component

(6)
$$\begin{bmatrix} [M_{11}] & \cdots & [M_{1n}] \\ \cdots & \cdots & \cdots \\ [M_{n1}] & \cdots & [M_{nn}] \end{bmatrix} \begin{bmatrix} \{\ddot{D}_1\} \\ \cdots \\ \{\ddot{D}_n\} \end{bmatrix} + (\text{damping term}) + \begin{bmatrix} [K_{11}] & \cdots & [K_{1n}] \\ \cdots & \cdots & \cdots \\ [K_{n1}] & \cdots & [K_{nn}] \end{bmatrix} \begin{bmatrix} \{D_1\} \\ \cdots \\ \{D_n\} \end{bmatrix}$$
$$= -\begin{bmatrix} [M_{11}] & \cdots & [M_{1n}] \\ \cdots & \cdots & \cdots \\ [M_{n1}] & \cdots & [M_{nn}] \end{bmatrix} \left(\begin{bmatrix} \{E_{x1}\} \\ \cdots \\ \{E_{xn}\} \end{bmatrix} \ddot{D}_{x0} + \begin{bmatrix} \{E_{y1}\} \\ \cdots \\ \{E_{yn}\} \end{bmatrix} \ddot{D}_{y0} \right)$$
$$\{D_i\} = \begin{Bmatrix} D_{xi} \\ D_{yi} \\ \Theta_i \end{Bmatrix} \quad (i = 1 \sim n)$$

(7)
$$[M_{ij}] = m_{ij}[M_p], \quad [K_{ij}] = k_{ij}[K_p] \quad (i, j = 1 \sim n)$$
$$\{E_{xi}\} = e_{xi}\{E_{xp}\}, \quad \{E_{yi}\} = e_{yi}\{E_{yp}\} \quad (i = 1 \sim n)$$

(8) Planar Solution
$$(-{}_s\Omega_p^2[M_p] + [K_p])\{{}_sU_p\} = \{0\}$$
$${}_s\beta_{xp} = \lfloor {}_sU_p \rfloor [M_p]\{E_{xp}\} / \lfloor {}_sU_p \rfloor [M_p]\{{}_sU_p\}$$
$${}_s\beta_{yp} = \lfloor {}_sU_p \rfloor [M_p]\{E_{yp}\} / \lfloor {}_sU_p \rfloor [M_p]\{{}_sU_p\} \quad (s = 1 \sim 3)$$

Axial Solution $[M_a] = (m_{ij}),\ [K_a] = (k_{ij}),\ \{E_{xa}\} = (e_{xi}),\ \{E_{ya}\} = (e_{yi})$
$$(-{}_t\Omega_a^2[M_a] + [K_a])\{{}_tU_a\} = \{0\}$$
$${}_t\beta_{xa} = \lfloor {}_tU_a \rfloor [M_a]\{E_{xa}\} / \lfloor {}_tU_a \rfloor [M_a]\{{}_tU_a\}$$
$${}_t\beta_{ya} = \lfloor {}_tU_a \rfloor [M_a]\{E_{ya}\} / \lfloor {}_tU_a \rfloor [M_a]\{{}_tU_a\} \quad (t = 1 \sim n)$$
$$\{{}_tU_a\} = ({}_tu_i)$$

(9)
$$\left(-{}_s\Omega_p^2\,{}_t\Omega_a^2 \begin{bmatrix} [M_{11}] & \cdots & [M_{1n}] \\ \cdots & \cdots & \cdots \\ [M_{n1}] & \cdots & [M_{nn}] \end{bmatrix} + \begin{bmatrix} [K_{11}] & \cdots & [K_{1n}] \\ \cdots & \cdots & \cdots \\ [K_{n1}] & \cdots & [K_{nn}] \end{bmatrix} \right) \begin{bmatrix} {}_tu_1\{{}_sU_p\} \\ \cdots \\ {}_tu_n\{{}_sU_p\} \end{bmatrix} = \{0\}$$

x component of participation factor $= {}_s\beta_{xp}\,{}_t\beta_{xa}$

y component of participation factor $= {}_s\beta_{yp}\,{}_t\beta_{ya}$ $(s = 1 \sim 3,\ t = 1 \sim n)$

(10) $\begin{Bmatrix} \ddot{D}_{x0}(t) \\ \ddot{D}_{y0}(t) \end{Bmatrix}$: two-dimensional white noise uncorrelated between major and minor components

i. e.
$$\begin{bmatrix} E[\ddot{D}_{x0}(t_1)\ddot{D}_{x0}(t_2)] & E[\ddot{D}_{x0}(t_1)\ddot{D}_{y0}(t_2)] \\ E[\ddot{D}_{y0}(t_1)\ddot{D}_{x0}(t_2)] & E[\ddot{D}_{y0}(t_1)\ddot{D}_{y0}(t_2)] \end{bmatrix} = \begin{bmatrix} I_{xx} & I_{xy} \\ I_{xy} & I_{yy} \end{bmatrix} \delta(t_1 - t_2)$$

$E[\cdot\cdot]$: operator of ensemble average for stationary process

with
$$\begin{bmatrix} I_{xx} & I_{xy} \\ I_{xy} & I_{yy} \end{bmatrix} = \begin{bmatrix} \cos\phi & -\sin\phi \\ \sin\phi & \cos\phi \end{bmatrix} \begin{bmatrix} I_{max} & 0 \\ 0 & I_{min} \end{bmatrix} \begin{bmatrix} \cos\phi & \sin\phi \\ -\sin\phi & \cos\phi \end{bmatrix}$$

I_{max} : intensity of white noise in major component

I_{min} : intensity of white noise in minor component

ϕ : orientation angle of major axis measured from x axis

(11)
$$\begin{bmatrix} E[|d_x(x,y,t)|^2] & E[d_x(x,y,t)\,d_y(x,y,t)] \\ E[d_x(x,y,t)\,d_y(x,y,t)] & E[|d_y(x,y,t)|^2] \end{bmatrix} = I_{xx}[R_{xx}(x,y)] + 2I_{xy}[R_{xy}(x,y)] + I_{yy}[R_{yy}(x,y)]$$

where
$$[R_{xx}(x,y)] = \sum_i \sum_j a_{ij} \begin{Bmatrix} {}_i(\beta u)_{xx}(x,y) \\ {}_i(\beta u)_{yx}(x,y) \end{Bmatrix} \lfloor {}_j(\beta u)_{xx}(x,y) \quad {}_j(\beta u)_{yx}(x,y) \rfloor$$
$$[R_{xy}(x,y)] = \frac{1}{2} \sum_i \sum_j a_{ij} \left(\begin{Bmatrix} {}_i(\beta u)_{xx}(x,y) \\ {}_i(\beta u)_{yx}(x,y) \end{Bmatrix} \lfloor {}_j(\beta u)_{xy}(x,y) \quad {}_j(\beta u)_{yy}(x,y) \rfloor + \begin{Bmatrix} {}_i(\beta u)_{xy}(x,y) \\ {}_i(\beta u)_{yy}(x,y) \end{Bmatrix} \lfloor {}_j(\beta u)_{xx}(x,y) \quad {}_j(\beta u)_{yx}(x,y) \rfloor \right)$$
$$[R_{yy}(x,y)] = \sum_i \sum_j a_{ij} \begin{Bmatrix} {}_i(\beta u)_{xy}(x,y) \\ {}_i(\beta u)_{yy}(x,y) \end{Bmatrix} \lfloor {}_j(\beta u)_{xy}(x,y) \quad {}_j(\beta u)_{yy}(x,y) \rfloor$$
$$i, j = 1 \sim 3$$
$$a_{ij} = \frac{2({}_i\zeta\,{}_i\Omega + {}_j\zeta\,{}_j\Omega)}{4\,{}_i\Omega\,{}_j\Omega({}_i\zeta\,{}_i\Omega + {}_j\zeta\,{}_j\Omega)({}_j\zeta\,{}_i\Omega + {}_i\zeta\,{}_j\Omega) + ({}_i\Omega^2 - {}_j\Omega^2)^2}$$

(12)
$$E[|d_\psi(x,y,t)|^2] = \lfloor \cos\psi \quad \sin\psi \rfloor \begin{bmatrix} E[|d_x(x,y,t)|^2] & E[d_x(x,y,t)\,d_y(x,y,t)] \\ E[d_x(x,y,t)\,d_y(x,y,t)] & E[|d_y(x,y,t)|^2] \end{bmatrix} \begin{Bmatrix} \cos\psi \\ \sin\psi \end{Bmatrix}$$

where $d_\psi(x,y,t) = d_x(x,y,t)\cos\psi + d_y(x,y,t)\sin\psi$

: single component of the 2-D drift of $\begin{Bmatrix} d_x(x,y,t) \\ d_y(x,y,t) \end{Bmatrix}$ extracted in the direction of an angle ψ from x axis

(13)
$$[R_{xx}(x,y)] = \begin{bmatrix} A_1\bar{y}^2 - 2B_{21}\bar{y} + C_{11} & (\text{sym.}) \\ -A_1\bar{x}\bar{y} + B_{21}\bar{x} + B_{11}\bar{y} - C_{21} & A_1\bar{x}^2 - 2B_{11}\bar{x} + C_{31} \end{bmatrix}$$
$$[R_{xy}(x,y)] = \begin{bmatrix} -A_2\bar{y}^2 + 2B_{22}\bar{y} - C_{21} & (\text{sym.}) \\ A_2\bar{x}\bar{y} - B_{22}\bar{x} - B_{12}\bar{y} + C_{22} & -A_2\bar{x}^2 + 2B_{12}\bar{x} - C_{32} \end{bmatrix}$$
$$[R_{yy}(x,y)] = \begin{bmatrix} A_3\bar{y}^2 - 2B_{23}\bar{y} + C_{31} & (\text{sym.}) \\ -A_3\bar{x}\bar{y} + B_{23}\bar{x} + B_{13}\bar{y} - C_{32} & A_3\bar{x}^2 - 2B_{13}\bar{x} + C_{33} \end{bmatrix}$$

where
$$\begin{bmatrix} A_1 & A_2 & A_3 \\ B_{11} & B_{12} & B_{13} \\ B_{21} & B_{22} & B_{23} \\ C_{11} & C_{21} & C_{31} \\ C_{21} & C_{22} & C_{32} \\ C_{31} & C_{32} & C_{33} \end{bmatrix} = \sum_i \sum_j b_{ij} \begin{Bmatrix} 1 \\ {}_i\bar{e}_x \\ {}_i\bar{e}_y \\ {}_i\bar{e}_y\,{}_j\bar{e}_y \\ {}_i\bar{e}_x\,{}_j\bar{e}_y \\ {}_i\bar{e}_x\,{}_j\bar{e}_x \end{Bmatrix} \lfloor {}_i\bar{e}_y\,{}_j\bar{e}_y \quad \tfrac{1}{2}({}_i\bar{e}_x\,{}_j\bar{e}_y + {}_i\bar{e}_y\,{}_j\bar{e}_x) \quad {}_i\bar{e}_x\,{}_j\bar{e}_x \rfloor \quad (i, j = 1 \sim 3)$$
$$b_{ij} = a_{ij} / \{(1 + {}_i\bar{e}_x^2 + {}_i\bar{e}_y^2)(1 + {}_j\bar{e}_x^2 + {}_j\bar{e}_y^2)\}$$

(14)
$$E[|d_x(x,y,t)|^2] = A(\bar{y} - B_y/A)^2 + (C_{xx} - B_y^2/A)$$
$$E[d_x(x,y,t)\,d_y(x,y,t)] = -A(\bar{x} - B_x/A)(\bar{y} - B_y/A) - (C_{xy} - B_xB_y/A)$$
$$E[|d_y(x,y,t)|^2] = A(\bar{x} - B_x/A)^2 + (C_{yy} - B_x^2/A)$$

where
$$\begin{Bmatrix} A \\ B_x \\ B_y \\ C_{xx} \\ C_{xy} \\ C_{yy} \end{Bmatrix} = \begin{bmatrix} A_1 & A_2 & A_3 \\ B_{11} & B_{12} & B_{13} \\ B_{21} & B_{22} & B_{23} \\ C_{11} & C_{21} & C_{31} \\ C_{21} & C_{22} & C_{32} \\ C_{31} & C_{32} & C_{33} \end{bmatrix} \begin{Bmatrix} I_{xx} \\ -2I_{xy} \\ I_{yy} \end{Bmatrix}$$

(15)
$$\begin{bmatrix} E[|d_x(x,y,t)|^2] & E[d_x(x,y,t)\,d_y(x,y,t)] \\ E[d_x(x,y,t)\,d_y(x,y,t)] & E[|d_y(x,y,t)|^2] \end{bmatrix} \equiv a_{11} \begin{bmatrix} I_{xx} & I_{xy} \\ I_{xy} & I_{yy} \end{bmatrix}$$

when $K_{wx} = K_{wy} = 0$

TENSORIAL NATURE OF RESPONSE DRIFT

With a view to obtaining better insight into the fundamental characteristics of response drift, an overly approximated but practically useful idealization of ground motions is taken up. This is a three-parameter family of 2-D white noise uncorrelated between its major and minor components in Art. (10). Then it can be shown that the expectancy relationship of Art. (11) holds for the amplitudes of 2-D drift during stationary elastic response. Obviously the left-side set of ensemble averages defines a tensor on the horizontal plane, from which the expectancy of amplitude in any direction is sufficiently determined by the formula in Art. (12). Three symmetric matrices in the right side of Art. (11) ($[R_{xx}]$, $[R_{xy}]$ and $[R_{yy}]$) embody the pointwise system properties of torsional response, rendered independent of the excitation. Use of the expression of participation functions in Art. (5) leads then to a more explicit representation

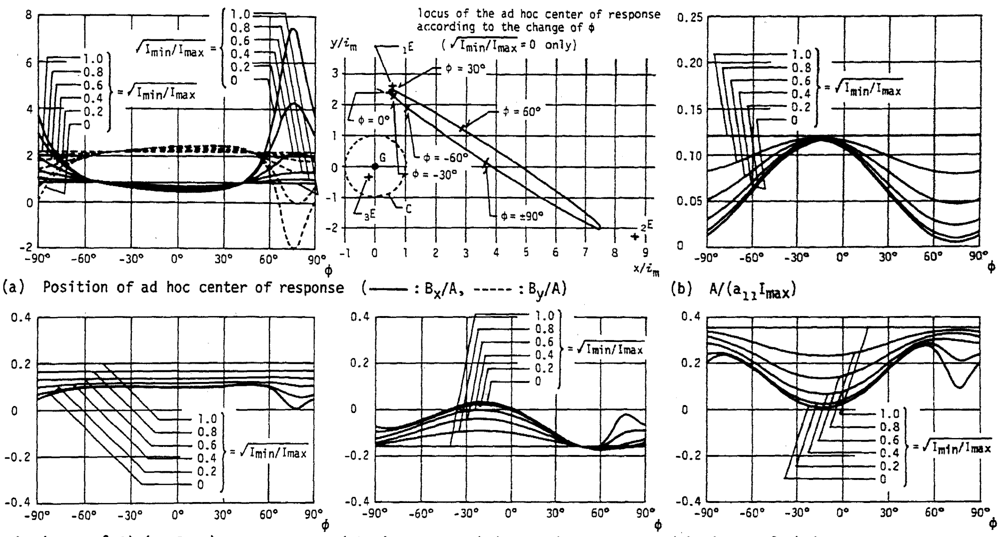

(a) Position of ad hoc center of response (—— : B_x/A, ----- : B_y/A)

(b) $A/(a_{11}I_{max})$

(c) $(C_{xx} - B_y^2/A)/(a_{11}I_{max})$

(d) $(C_{xy} - B_xB_y/A)/(a_{11}I_{max})$

(e) $(C_{yy} - B_x^2/A)/(a_{11}I_{max})$

Figure 3

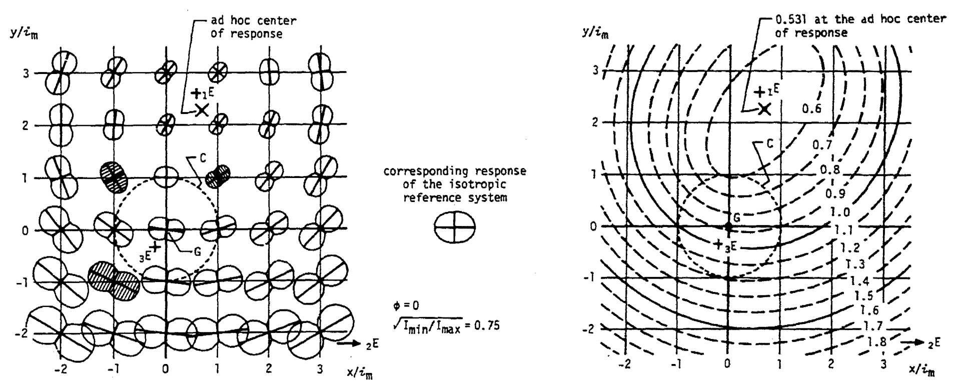

(a) Planar distribution of $\sqrt{E[|d_\psi(x,y,t)|^2]}$ at sampling points

(b) Contour of $\sqrt{\underset{-\pi \le \psi \le +\pi}{\mathrm{Max}} \{E[|d_\psi(x,y,t)|^2]\}/(a_{11}I_{max})}$

Figure 4

of these matrices in the form of Art. (13). Eliminating the separable factor of the position of response evaluation, a set of fifteen system parameters (A_i, B_{ij} and C_{ij}) becomes relevant to the current formulation.

The above results provide a compact expression of Art. (14) for the three components of the expectancy tensor of 2-D drift. Their pointwise distribution is quadratic, indicating the existence of an ad hoc center of response and with the parameters of A, B_x, B_y, C_{xx}, C_{xy} and C_{yy} related simply to the 2-D characteristics of excitation. Using the same example of torsional system as in Fig. 2, dependence of these parameters upon the orientation of major axis and the role of minor-axis component is examined in Fig. 3. Removal of "concentrated eccentric stiffness" from the example system, thus resulting in a triple eigenvalue associated with K_0 and in ideally translational 2-D response, offers a normalizing factor for the present illustration [vide Art. (15)]. Tendency of 2-D excitation confined in a single direction is seen there to accompany more pronounced dependence on its orientation. Singularities appear when nearly unidirectional excitation acts along the line through G and ${}_1E$, influenced directly by the diminishing contribution of the fundamental mode. Effects of the modal participation are most strikingly evidenced by the locus of ad hoc center of response included in the figure. However such extreme instances may be practically unimportant, since most of significant strong-motion records have had stronger trend of planar sprawl with over 50 % amplitude in minor-axis component (e. g., Ref. 1).

Fig. 4 illustrates the distribution of response drift, using the same example and specifying the orientation of major axis and the relative contribution of minor-axis component. Part (a) is intended to display the 2-D nature of drift by means of the preceding formula of Art. (12). Comparison among the sampling points clarifies more involved response near ${}_1E$, affected considerably by higher modes. More distant from ${}_1E$, the response tends to become simpler reflecting the dominant role of twist in the fundamental mode. The latter is related to severely necked shape of the 2-D drift despite the sprawled shape for the excitation and the response of the reference system. When noting only the maximum directional amplitude of drift, the contour plot of part (b) is obtained. Its normalizing factor is again the corresponding drift of the reference system,

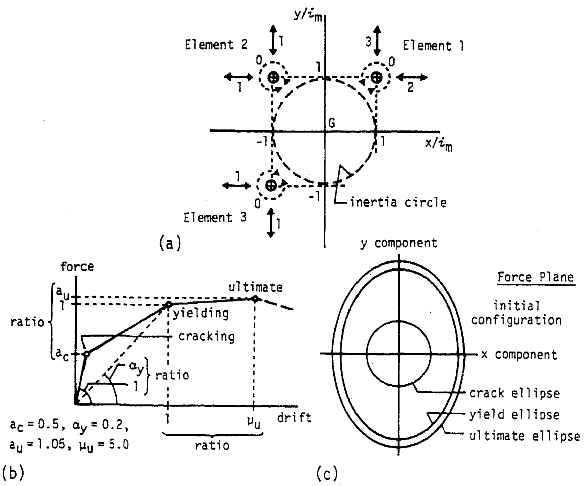

1. Geometry for the configuration of restoring force elements ⟶ (a).
2. Elastic stiffness of the elements; orientation of principal axes, and relative values among them and between their principal axes ⟶ (a). The absolute values are determined so as to realize an elastic fundamental period of 0.3 sec for the combined system. Stiffness-proportional damping is assumed with a 5 % viscous damping factor in elastic response.
3. Restoring force characteristics of the elements; uniaxial skeleton properties of the elements along their principal axes ⟶ (b). The degrading law of hysteresis is associated with this. Then a two-dimensional interpretation is used on the basis of cracking, yielding and ultimate criteria on the force plane ⟶ (c).
4. Total yielding strength of the system, Ay, is assumed to be identical between x and y axes. This is shared, in each direction, by the elements in proportion to their elastic stiffness.
5. Ground shaking; Holiday Inn record (1st floor, 8244 Orion Boulevard, Los Angeles, San Fernando EQ in Southern Calif., Feb. 9, 1971), N00W and S90W components used as the x and y components of excitation, respectively, and with a modified peak amplitude of A_{max} in its major component.

Figure 5 Specification of example problem hence the numeral being interpreted as the increasing factor of drift caused by the effects of torsion. The contour gives an inclined ellipse around the ad hoc center of response, tending to be circular with longer distance from the point.

FAILURE OF YIELDING AND HYSTERETIC STRUCTURE

Results of an example calculation are shown for understanding significant features observed in the combined lateral and torsional failure of yielding and hysteretic systems under the action of 2-D ground motions. Specification of the system and the excitation examined herein can be found in Fig. 5. Consisting of three discrete restoring elements, composition of their elastic stiffness results in the same properties of total system as those used in the foregoing Figs. 2, 3 and 4. Moreover the orientation of major axis and the relative share of minor-axis component specified in Fig. 4 turn out to be nearly consistent with the excitation, when replacing the expectancy of the product of amplitudes by the

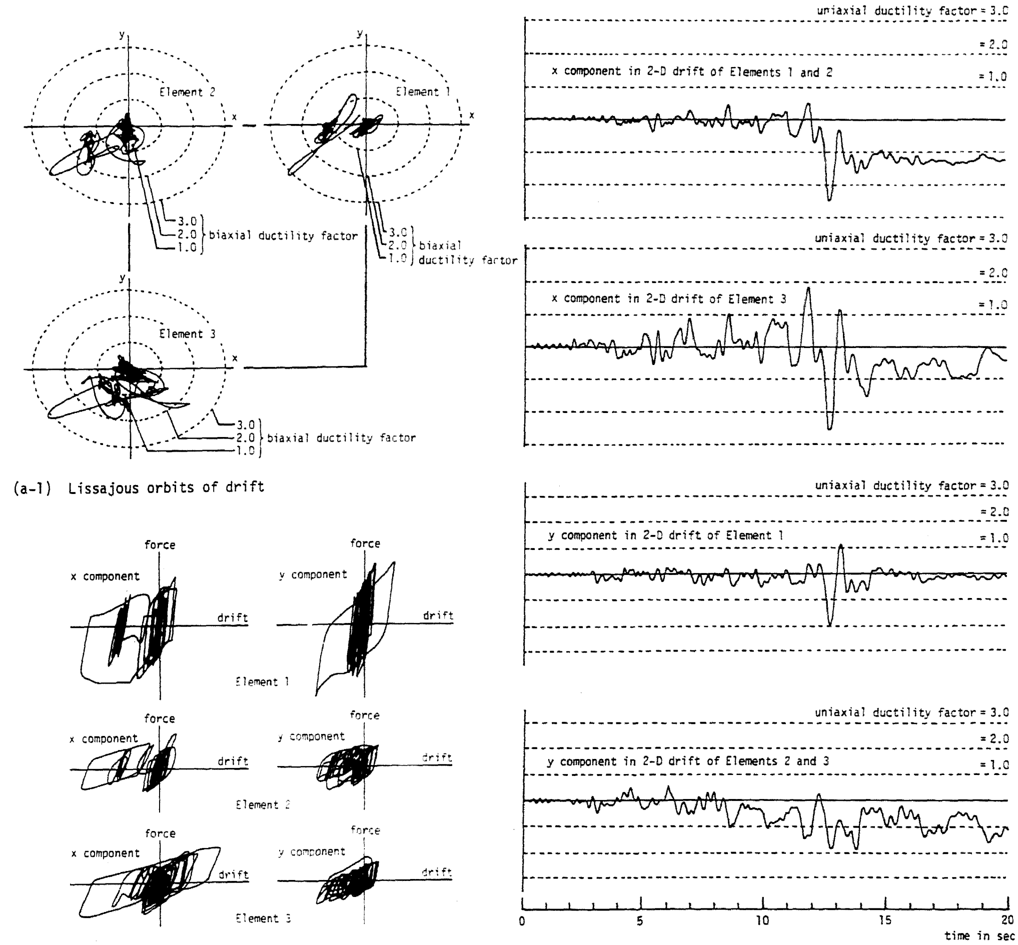

(a-1) Lissajous orbits of drift

(a-2) Component representation of restoring force relations

(a-3) Time-histories of drift

(a) $A_{max}/A_y = 1.2$

Figure 6-(a)

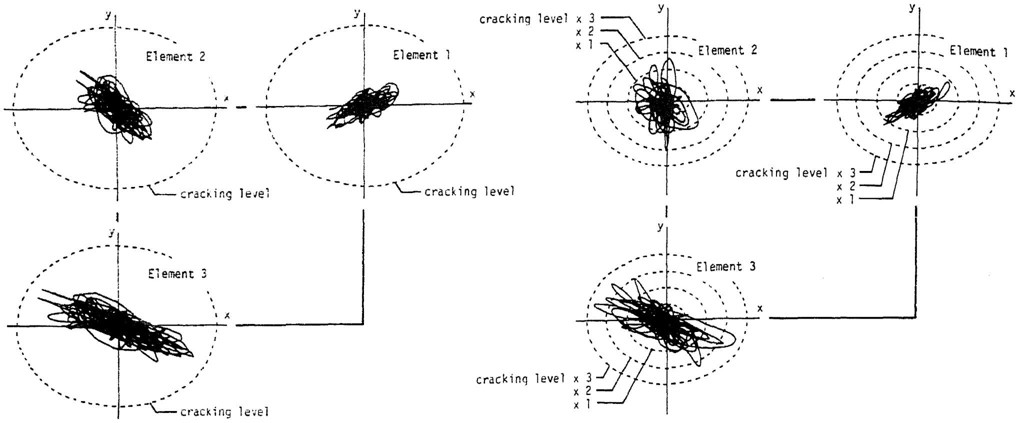

(b) Lissajous orbits of drift for $A_{max}/A_y = 0.1$

(c) Lissajous orbits of drift for $A_{max}/A_y = 0.5$

Figure 6-(b), (c)

corresponding integral over the entire time axis. Therefore its fundamental properties are evident from these figures, hatching in Fig. 4-(a) indicating the 2-D drifts of the current concern. The absolute value of stiffness is so designed as to provide a fundamental period of 0.3 sec for the system.

Restoring force relations of the individual elements are characterized in the two dimensions of horizontal plane. Restricted to uniaxial loading along their principal axes, the relations reduce to the degrading quadrilinear law for reinforced concrete. The latter allows to take account of the degrading capacity of hysteretic energy loss and the deteriorating ductility far beyond yield point, in addition to the softening due to cracking and yielding. By use of a phenomenological analogy with the stress-strain plasticity theory in the solid mechanics, the 2-D formulation resorts to a certain set of hardening and flow rules on the force plane. Its mathematical details have appeared in Refs. 2 and 3.

For the total system, an identical yielding strength expressed as an acceleration, A_y, is assumed between its principal axes. Also the peak acceleration in major-axis component, A_{max}, is used to stand for the strength of 2-D excitation. Then the 2-D drifts of individual elements become a matter of specific interest, normalized in terms of ductility factor and related to the relative strength of A_{max}/A_y. Fig. 6 summarizes the results of analysis along this line. Part (a) contains an instance featured by noticeably developed yielding, while additional parts of (b) and (c) supplement a totally elastic instance and a cracked but unyielded instance, respectively. By comparisons, the 2-D modes of drift are seen to differ markedly according to the different levels of response. This suggests the location of effective center of twist can vary significantly with the progress of cracking and yielding. For instance, the case of part (a) exhibits a trend of translational drift along the peak locus. Closer examinations and their design implications will be reported elsewhere.

REFERENCES

1. H. Takizawa, "Destructive capability of extreme earthquake motions examined in two dimensions of horizontal plane," *Proc. 7th Wld Conf. Earthq. Eng.*, Istanbul, Sept. 1980, Vol. 2, pp. 365-372.
2. H. Takizawa and H. Aoyama, "Biaxial effects in modelling earthquake response of R/C structures," *Earthq. Engng Struct. Dyn.*, Vol. 4, No. 6, Oct. 1976, pp. 523-552.
3. H. Takizawa, "Biaxial and gravity effects in modeling strong-motion response of R/C structures," *Proc. 6th Wld Conf. Earthq. Eng.*, New Delhi, Jan. 1977, Vol. II, pp. 1022-1027.